Microcavity Effect of Top-emission Organic Light-emitting Diodes Using Aluminum Cathode and Anode

Chang-Jun Lee, Young-Il Park, Jang-Hyuk Kwon,[†] and Jong-Wook Park[*]

Department of Chemistry/Display Research Center, The Catholic University of Korea, Bucheon 420-743, Korea
[*]E-mail: hahapark@catholic.ac.kr
[†]Department of Information Display, Kyung Hee University, Seoul 130-701, Korea
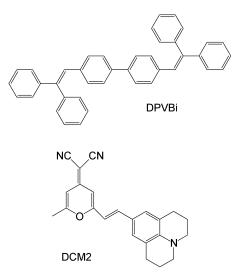*Received March 5, 2005*

We report microcavity effect of top emission organic light-emitting diodes (OLEDs) by using Al cathode and anode, which are feasible for not only top emission EL and angle dependant effects but facile evaporation process without ion sputtering. The device in case of Alq₃ green emission showed largely shifted EL maximum wavelength as 650 nm maximum emission. It was also observed that detection angle causes different EL maximum wavelength and different CIE values in R, G, B color emission. As a result, the green device using Alq₃ emission showed 650 nm emission (0°) to 576 nm emission (90°) as detection angle changed. We believe that these phenomena can be also explained with microcavity effect which depends on the different length of light path caused by detection angle.

Key Words : Electroluminescence, Top emitting, Microcavity, OLEDs

Introduction

Organic light-emitting diodes (OLEDs) have been the subject of intense research because of their promising application in full-color displays.[1-3] Active matrix OLEDs in general will be benefit from adopting top emitting OLEDs structure because all circuitry can be placed at the bottom without any interference from compounds such as wiring and transistor and aperture ratio can be increased.[4]

Top emitting OLEDs are composed of a reflective bottom electrode, organic layer, and a semitransparent top electrode for light out coupling. Conventional top electrodes are mostly consisted of transparent conducting oxides or thin metal films as well as their combination. These top electrodes show strong reflection due to large refractive index,

DPVBi

DCM2

Scheme 1. Chemical structure of 4,4′-bis-(2,2-diphenyl-vinyl)-biphenyl (DPVBi) and 4-dicyanomethylene-2-methyl-6-{2-(2,3,6,7-tetra-hydro-1H,5H-benzo[ij]quinolizin-8-yl]-4H-pyran (DCM2).

and lead to microcavity effect on emission characteristics of device. Such microcavity structures lead to spectral narrowing of the emission band, enhancements of the peak intensity and improved output.[5-8]

We report new top emission OLEDs configuration by using Al cathode and anode, which are feasible for top not only emission EL and angle dependant effects but facile evaporation process without ion sputtering.

Experimental Section

Tris-(8-hydroxyquinoline) aluminium (Alq3), N,N′-di-(naphthalen-1-yl)-N,N′-diphenyl-benzidine (NPB), 4,4′,4″-tris(N-(2-naphthyl)-N-phenyl-amino)-triphenylamine (2-TNATA) and 4,4′-bis-(2,2-diphenyl-vinyl)-biphenyl (DPVBi) were purchased from Sensient Co. and 4-dicyanomethylene-2-methyl-6-{2-(2,3,6,7-tetra-hydro-1H,5H-benzo [ij]quino-lizin-8-yl]-4H-pyran (DCM2) was purchased from Exciton. All materials were used without further purification unless otherwise note.

The devices were fabricated on glass substrates. The organic layer were vacuum-deposited using thermal evaporation at a vacuum base pressure of 5.0×10^{-6} Torr, the rate of deposition being 1 Å per second to give an emitting area of 9 mm² and aluminum layer was continuously deposited with same vacuum condition. The multilayer structure consists the following layers: Al as an anode (200 nm), 2-TNATA as a hole injection (60 nm), NPB as a hole transport layer (15 nm), emitting layer (EML), electron transport layer (ETL), LiF as an electron injection layer (1 nm), Al as a cathode (20 nm).

Perkin Elmer luminescence spectrometer LS55 (Xenon flash tube) was used for electroluminescence spectroscopy. Current-voltage(I-V) characteristics of the film in plane were measured using Keithley 2410 electrometer. Light intensity was obtained by Minolta CS-100.
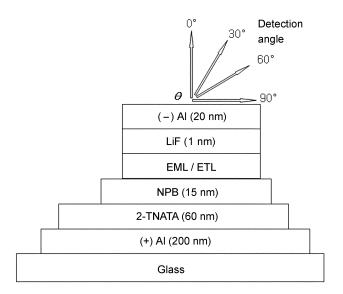
Figure 1. Configuration and detection angle of devices. EML/ETL thickness: green (Alq₃ 70 nm), red ((AlQ₃ + 3% DCM2) 30 nm/ Alq₃ 30 nm), blue (DPVBi 30 nm/Alq₃ 30 nm).
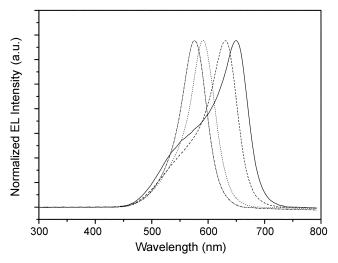

Figure 2. Normalized EL spectra of green device, Al(200 nm)/2-TNATA (60 nm)/NPB(15 nm)/Alq₃(70 nm)/LiF(1 nm)/Al(20 nm). Detection angle: (———): 0°, (- - -): 30°, (·····): 60°, (-·—·-): 90°.

Result and Discussion

The devices were designed to realize top emission in organic light-emitting diodes (OLEDs). The devices consist of reflective aluminum anode of 200 nm thickness and semitransparent aluminum cathode with thin thickness, 20 nm. Figure 1 shows configuration of device and different detection angles as 0°, 30°, 60°, 90°.

We fabricated three kinds of devices with the three primary emission color R, G, B. Figure 2 shows normalized EL spectra of device based on green emitter, Al(200 nm)/2-TNATA(60 nm)/NPB(15 nm)/Alq₃(70 nm)/LiF(1 nm)/Al(20 nm) under 33 V. EL spectra were observed as different angle way and 0° means detection of the front side of OLEDs device. In case of 0° detection, EL maximum wavelength appeared at 650 nm of red color region in spite of green Alq₃
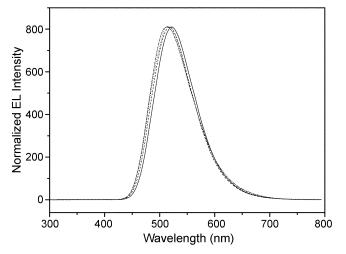

Figure 3. Normalized EL spectra of conventional green device, ITO/2-TNATA (60 nm)/NPB(15 nm)/Alq₃(70 nm)/LiF(1 nm)/Al(20 nm). Detection angle: (———): 0°, (- - -): 30°, (·····): 60°, (-·—·-): 90°.

emitter and residual weak green emission at around 550 nm. Conventional Alq₃ OLEDs device shows EL maximum value at around 520 nm (Figure 3) and there is no remarkable change as different detection angle, therefore it is clear that EL maximum value is changed under the device condition. When we detected EL light as 0°, 30°, 60°, 90° angle way, EL spectra were blue-shifted from 650 nm to 576 nm and bandwidth of spectrum was narrowed. All of these might be due to deletion of green wavelength region from microcavity effect.

A Fabry-Pìrot cavity introduces the constructive interference condition which is defined by the equation (1):[9]

$$2nd \cos\theta = m\lambda \ (m = 1, 2...)   (1)$$

where m is an integer termed the order of interference, n is the refractive index of the medium between the two mirror, d is the spacing between two electrodes, and θ represents the emission angle in the cavity.

Equation (1) shows that the resonance wavelength λ decreases with an increase of θ in the range of 0° to 90°. This result and interpretation consist with the result of conventional top emitting device and ours.[10]

From the EL efficiency point of view, conventional Alq₃ OLEDs device shows EL efficiency of 6.7 cd/A at 10 mA/cm², but the proposed green device shows 0.11 cd/A efficiency at 10 mA/cm². This tendency happens at overall current density. Therefore, there is a considerable cut-off phenomena in green emission region.

Saito *et al.* also reported top emitting OLEDs device by using Mg/Ag as cathode and Ag or ITO as anode, which showed weaker emission in comparison with the common device.[9]

Normalized EL spectra of device under applied voltage of 33 V, Al(200 nm)/2-TNATA(60 nm)/NPB(15 nm)/Alq₃ + 3%DCM2_(30 nm)/Alq₃(30 nm)/LiF(1 nm)/Al(20 nm), containing red emitter, Alq₃+DCM2 are shown in Figure 4. While the conventional device having DCM2 dopant shows
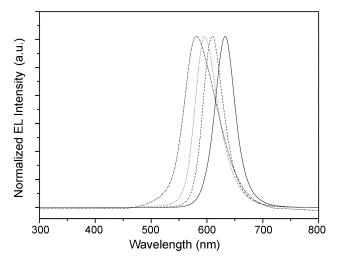
Figure 4. Normalized EL spectra of red device, Al(200 nm)/2-TNATA(60 nm)/NPB(15 nm)/Alq$_3$ + 3% DCM2_(30 nm)/Alq$_3$(30 nm)/LiF (1 nm)/Al(20 nm). Detection angle: (——): 0°, (- - -): 30°, (· · · · ·): 60°, (-· —·-) 90°.

Figure 5. EL spectra of blue device, Al(200 nm)/2-TNATA(60 nm)/NPB(15 nm)/DPVBi(30 nm)/Alq$_3$(30 nm)/LiF(1 nm)/Al(20 nm). Detection angle: (——): 0°, (- - -): 30°, (· · · · ·): 60°, (-· —·-): 90°.

Table 1. The EL peak wavelength as detection angles in the devices

EL maximum wavelength	θ(0°)	θ(30°)	θ(60°)	θ(90°)
Green device	650 nm	631 nm	591 nm	576 nm
Red device	632 nm	609 nm	596 nm	580 nm
Blue device	465 nm, 630 nm	466 nm, 592 nm	465 nm, 560 nm	465 nm, 552 nm

Table 2. CIE coordinate values of EL spectra as detection angles in the devices

CIE value	θ(0°)	θ(30°)	θ(60°)	θ(90°)
Green device	(0.556, 0.423)	(0.537, 0.444)	(0.515, 0.472)	(0.496, 0.487)
Red device	(0.670, 0.328)	(0.656, 0.343)	(0.582, 0.417)	(0.534, 0.465)
Blue device	(0.303, 0.307)	(0.332, 0.333)	(0.314, 0.447)	(0.249, 0.529)

EL maximum value at 611 nm and full bandwidth at half maximum(FWHM) of 76 nm, the proposed device using DCM2 dopant exhibits 632 nm EL emission and 42 nm FWHM value. As the detection angle increased in this device, EL spectrum was also blue-shifted and FWHM was broader from 42 nm to 69 nm. Especially, red color coordinate value (CIE) was improved from x = 0.624 and y = 0.374 of conventional device (0° angle way) to x = 0.670 and y = 0.328 under the device condition (0° angle way). This improvement is due to red-shifted EL maximum value from 611 nm to 632 nm and narrowed FWHM from 76 nm to 42 nm. We believe that these phenomena can be also explained by microcavity effect, which depends on the different length of light path caused by detection angle.

Blue device under 26 V, Al(200 nm)/2-TNATA(60 nm)/NPB(15 nm)/DPVBi(30 nm)/Alq$_3$(30 nm)/LiF(1 nm)/Al(20 nm), shows two EL maximum peaks at blue region and yellow ~ red region as shown in Figure 5. As the increased detection angle, the intensity of blue peak was relatively decreased and red peak was slightly increased and blue-shifted. To our knowledge these peak values due to microcavity effect are changed with the length of light path, refractive index, and detection angle.

We summarized EL peak wavelength and CIE values data in Table 1 and 2.

Further studies on these kinds of devices with different thickness and color are underway.

References

1. Tang, C. W.; Van Slyke, S. A.; Chen, C. H. *J. Appl. Phys.* **1989**, *65*, 3610.
2. Strukjelj, M.; Jordan, R.; Dodabalapur, A. *J. Am. Chem. Soc.* **1996**, *118*, 1213.
3. Adachi, C.; Tsutsui, T.; Saito, S. *Appl. Phys. Lett.* **1989**, *55*, 1489.
4. Hung, L. S.; Tang, C. W.; Mason, M. G.; Raychaudhuri, P.; Madathil, J. *Appl. Phys. Lett.* **2001**, *78*, 544.
5. Fisher, T. A.; Lidzey, D. G.; Pate, M. A.; Weaver, M. S.; Whittaker, D. M.; Skolnick, M. S.; Bradley, D. D. C. *Appl. Phys. Lett.* **1995**, *67*, 1355.
6. Jordan, R. H.; Rothberg, L. J.; Dodabalapur, A.; Slusher, R. E. *Appl. Phys. Lett.* **1996**, *69*, 1997.
7. Riel, H.; Kang, S.; Beierlein, T.; Ruhstaller, B.; Rieβ, W. *Appl. Phys. Lett.* **2003**, *82*, 466.
8. Han, S.; Feng, X.; Lu, Z. H.; Johnson, D.; Wood, R. *Appl. Phys. Lett.* **2003**, *82*, 2715.
9. Takada, N.; Tsutsui, T.; Saito, S. *Appl. Phys. Lett.* **1993**, *63*, 2032.
10. Jean, F.; Mulot, J.; Geffroy, B.; Denis, C.; Cambon, P. *Appl. Phys. Lett.* **2002**, *81*, 1717.